Review

Journal of Vibration and Control
2023, Vol. 0(0) 1–13

DOI: 10.1177/10775463231223271
journals.sagepub.com/home/jvc
Sage

Active suspension H_∞/generalized H_2 static output feedback control

Zhuqing Shi[1], Ruili Cao[2], Shishuo Zhang[1], Jie Guo[1], Shuyou Yu[1,3], and Hong Chen[1,4]

Abstract

This paper proposes an approach of H_∞/generalized H_2 (GH_2) static output feedback control for vehicle active suspension. To address the conflicting performance requirements in active suspension, the H_∞ norm is minimized to optimize the ride comfort performance, while the GH_2 norm is designed to meet time-domain hard constraints, including suspension stroke, road-holding performance, and actuator saturation. As not all states of active suspension are measurable in practice, the static output feedback control is designed using suspension stroke and sprung mass velocity as feedback signals. An invertible matrix condition is introduced in the static output feedback control design, which transforms the control problem into a convex optimization problem that can be solved using linear matrix inequalities (LMIs). Simulation and hardware-in-the-loop (HiL) experiments are conducted on both bump and random road responses for active and passive suspension of a 2-degree-of-freedom quarter vehicle. The proposed active suspension H_∞/GH_2 static output feedback controller is compared with H_∞ state feedback controller and the existing controller solved by LMIs and genetic algorithms (GAs), demonstrating that the proposed strategy achieves better ride comfort performance under various road conditions while satisfying all time-domain hard constraints.

Keywords

active suspension, H_∞/GH_2 control, static output feedback control, HiL experiment

1. Introduction

Vehicle suspension control is a complex multi-objective control problem (Chen et al., 2003). The control objectives involve conflicting performance requirements, such as maximizing ride comfort, limiting suspension stroke, enhancing road-holding capacity, and satisfying actuator saturation constraints (Deshpande et al., 2017). Among these objectives, optimizing ride comfort is particularly crucial.

Compared to passive and semi-active suspension systems (Tseng and Hrovat, 2015), active suspension introduces an additional active force between the vehicle body and tires (Wang et al., 2019). The active force is generated by the actuator of active suspension system, which can effectively suppress vibrations caused by road disturbances and improve the overall performance of the vehicle (Park and Yim, 2021). In recent years, significant efforts have been devoted to the development of active suspension systems.

Optimal control is available for addressing the multi-objective control problem in active suspension, such as the techniques including Linear Quadratic Regulator (LQR) (Taghirad and Esmailzadeh, 1998), Linear Quadratic Gaussian (LQG) (Zhang et al., 2022), Model Predictive Control (MPC) (Song and Wang, 2020; Theunissen et al., 2020), etc. The controllers of LQR and LQG are often designed to optimize conflicting performance requirements in a single objective function, in which determining the weighting metrics is challenging (Chen and Guo, 2005).

Robust control is another crucial method for active suspension control, which includes state feedback control

[1]Department of Control Science and Engineering, Jilin University, Changchun, China
[2]System Integration R&D Department, CRRC Zhuzhou Electric Co. Ltd., Zhuzhou, China
[3]College of Automation, Chongqing University of Posts and Telecommunications, Chongqing, China
[4]College of Electronics and Information Engineering, Tongji University, Shanghai, China

Received: 30 June 2023; accepted: 8 December 2023

Corresponding author:
Shuyou Yu, Department of Control Science and Engineering, Jilin University, Nanhu Road 5372, Mail box 9, Changchun 130025, China. College of Automation, Chongqing University of Posts and Telecommunications, Chongqing 400065, China.
Email: shuyou@jlu.edu.cn

and output feedback control. State feedback control requires full measurability of system states, which is difficult to implement in practical systems (Akbari et al., 2010; Du and Zhang, 2007; Li et al., 2019; Wei et al., 2020). Although the approach based on state observer can reconstruct state quantities, it has some disadvantages such as high implementation costs, complex system design, and significant observation errors (Du et al., 2020). In contrast, output feedback control employs the output signal that can be directly measured as the feedback quantity.

Static output feedback control is widely used in practice due to its low cost and simple structure (Goyal et al., 2023; Kim et al., 2023). A static output feedback controller has been designed based on the H_2 norm of a vehicle quarter active suspension, which uses the displacement and velocity of the suspension stroke as output feedback (Camino et al., 1999). An H_∞ static output feedback controller of the half-vehicle active suspension has been designed (Wei et al., 2018). The driver seat acceleration, as well as the vehicle body acceleration and pitch acceleration, are simultaneously minimized to improve ride comfort. In the research above, either the H_∞ norm or the H_2 norm is utilized to minimize multiple performance requirements in a single objective function. The solution to the control problem often comes with a certain degree of conservatism.

To reduce the conservatism of minimizing multiple performance requirements in a single objective function, the combination of H_∞ and generalized H_2 (GH_2) has been utilized for multi-objective functional control (Du and Zhang, 2008; Liu and Zhao, 2009). The H_∞ norm is employed to describe the performance index of ride comfort, while the GH_2 norm is designed to represent time-domain constraints. A suboptimal H_∞/GH_2 static output feedback control approach has been proposed based on linear matrix inequalities (LMIs) and genetic algorithms (GAs) (Du and Zhang, 2008). By using GAs to search for possible control gain matrices and then resolving the LMIs together with the minimization optimization problem, H_∞/GH_2 static output feedback controllers are obtained. Numerical simulations demonstrate that the proposed approach can achieve similar active suspension performance compared with the state feedback control case. An H_∞/GH_2 static output feedback controller for active suspension has been developed utilizing the suspension stroke as the feedback signal (Liu and Zhao, 2009). By employing a differential evolutionary algorithm to determine the control gain, the H_∞ performance is achieved while considering GH_2 constraints. Although different searching algorithms are used to address the bilinear matrix inequality (BMI) in static output feedback control, obtaining a global optimal solution is not guaranteed due to the non-convex nature of the BMI problem.

This paper proposes an approach of H_∞/GH_2 static output feedback control that achieves the global optimal solution. The ride comfort is improved by optimizing an H_∞ norm, while a GH_2 norm is used to describe time-domain constraints such as suspension stroke, road-holding performance, and actuator saturation. To transform the control problem into a convex optimization problem, an invertible matrix condition is introduced for static output feedback control design. The global optimal solution of the H_∞/GH_2 static output feedback control law can then be solved using LMIs. The suspension stroke and vertical velocity of the vehicle body are chosen as output feedback signals. The proposed approach is compared with H_∞ state feedback control and an existing approach that obtains control gain matrices based on LMIs and GAs. Simulation and hardware-in-the-loop (HiL) experiments are conducted on both random and deterministic road surfaces, demonstrating that the proposed approach achieves better performance with simplified techniques.

This paper is organized as follows: Section 2 sets up the control problem based on the 2-degree-of-freedom (2-DOF) vehicle quarter suspension model, Section 3 designs the H_∞/GH_2 static output feedback controller for the active suspension, Section 4 presents comparative simulation and HiL experiments to demonstrate the superiority of the proposed approach, and Section 5 provides the conclusion.

Notation: $\mathbb{R}^n$ represents the n-dimensional Euclidean space, $\mathbb{R}^{n\times m}$ denotes the set of all $n \times m$ real matrices, $\|\cdot\|$ denotes the matrix 2-norm or the Euclidean vector norm, $\|G\|_\infty$ is H_∞ norm of transfer function G. For a real symmetric matrix Q, $Q > 0$ indicates that the matrix is positive definite, rank(Q) denotes the rank of the matrix Q, # denotes the transpose of a matrix block at a symmetric position, and I is a unit matrix of appropriate dimensions.

2. Problem setup

In this section, an active suspension model based on a 2-DOF quarter vehicle is established. Then the performance requirements and time-domain constraints are introduced. Finally, the control objective is proposed.

2.1. Suspension system modeling

In this subsection, both active suspension and passive suspension are established based on a 2-DOF quarter vehicle, in which the impact of vehicle load transfer on the suspension system is ignored (Gordon et al., 1991).

The diagrams of passive and active suspensions are shown in the left and right parts of Figure 1, respectively. The vehicle body mass is represented by the sprung mass m_s, and the tire is reduced to an elastic element with unsprung mass m_u and stiffness k_u. The passive suspension is simplified approximately to a linear spring and damping element between the sprung mass and unsprung mass, where the spring stiffness and the damping coefficient are k_s and c_s, respectively.

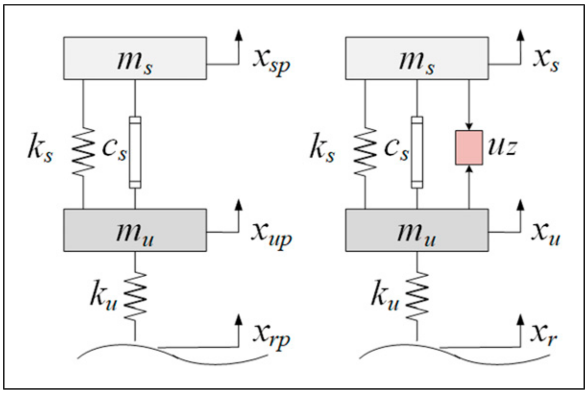

Figure 1. The diagrams of passive and active suspension.

The passive suspension dynamics can be expressed as

$$\begin{cases} m_s\ddot{x}_{sp} = -k_s\left(x_{sp} - x_{up}\right) - c_s\left(\dot{x}_{sp} - \dot{x}_{up}\right), \\ m_u\ddot{x}_{up} = k_s\left(x_{sp} - x_{up}\right) + c_s\left(\dot{x}_{sp} - \dot{x}_{up}\right) - k_u\left(x_{up} - x_{rp}\right), \end{cases} \tag{1}$$

where x_{sp}, x_{up}, and x_{rp} denote the vertical displacements of sprung mass, unsprung mass, and road surface, respectively. In (1), the expressions $x_{sp} - x_{up}$ and $x_{up} - x_{rp}$ represent the suspension stroke and tire deflection, the variables $\dot{x}_{sp}$ and $\dot{x}_{up}$ denote the velocity of the sprung mass and unsprung mass, respectively.

The active suspension (right in Figure 1) introduces an extra actuator (red block) based on the passive suspension. The actuator generates an active force u_z, which is the control input and acts on both sprung and unsprung mass. Based on Newton's second law of motion, the dynamics of active suspension can be represented as

$$\begin{cases} m_s\ddot{x}_s = -k_s(x_s - x_u) - c_s(\dot{x}_s - \dot{x}_u) + u_z, \\ m_u\ddot{x}_u = k_s(x_s - x_u) + c_s(\dot{x}_s - \dot{x}_u) - k_u(x_u - x_r) - u_z, \end{cases} \tag{2}$$

where the variables x_s, x_u, and x_r denote the vertical displacements of sprung mass, unsprung mass, and road surface, respectively. The suspension stroke and tire deflection are represented by $x_s - x_u$ and $x_u - x_r$, respectively. And the velocity of sprung mass and unsprung mass are $\dot{x}_s$ and $\dot{x}_u$, respectively.

2.2. Performance requirements

The performance requirements for suspension design mainly include ride comfort, suspension stroke limit, road-holding, and actuator saturation. The evaluation index of ride comfort is the vertical acceleration of the vehicle body, that is, $\ddot{x}_s$. And the root mean square (RMS) value of $\ddot{x}_s$ is introduced to evaluate ride comfort (Chen and Guo, 2005), that is

$$RMS(\ddot{x}_s) = \sqrt{\frac{1}{N}\sum_{i=1}^{N}|\ddot{x}_s|^2} \tag{3}$$

where N is the total number of sampling points.

Suspension stroke represents the relative displacement of the vehicle body and tires. When the suspension stroke exceeds a maximum value $S_{\max}$, it will cause damage to the suspension and reduce the ride comfort. Therefore, the suspension stroke should be constrained as

$$\frac{|x_s - x_u|}{S_{\max}} \le 1 \tag{4}$$

Road-holding performance affects handling capacity of vehicle, the ground cannot provide sufficient tire force when the dynamic tire load $k_u(x_u - x_r)$ is greater than the static tire load $(m_s + m_u)g$. So the ratio of dynamic tire load and static tire load (named as tire dynamic-to-static load ratio) should satisfy

$$\frac{k_u(x_u - x_r)}{(m_s + m_u)g} \le 1 \tag{5}$$

In addition, the active force u_z should satisfy the actuator saturation constraint

$$\frac{|u_z|}{u_{z\max}} \le 1 \tag{6}$$

where $u_{z\ \max}$ is the maximum value of $|u_z|$.

2.3. Control objective

Consider a system described by the state space equations

$$\begin{cases} \dot{x}(t) = Ax(t) + B_1\omega(t) + B_2u(t), \\ z_1(t) = C_1x(t) + D_{11}\omega(t) + D_{12}u(t), \\ z_2(t) = C_2x(t) + D_{21}\omega(t) + D_{22}u(t), \\ y(t) = C_3x(t), \end{cases} \tag{7}$$

where $x \in \mathbb{R}^{n_x}$ is the state vector, $\omega \in \mathbb{R}^{n_\omega}$ is the disturbance input vector, $u \in \mathbb{R}^{n_u}$ denotes the control input, $z_1 \in \mathbb{R}^{n_{z_1}}$ and $z_2 \in \mathbb{R}^{n_{z_2}}$ are the vectors of performance output and constrained output, respectively. The measured output vector is $y \in \mathbb{R}^{n_y}$ and the measured output matrix $C_3 \in \mathbb{R}^{n_y \times n_x}$ is with full rank of rows.

For the active suspension system, the state vector, road disturbance input, and control input in the system (7) are

$$x = \begin{bmatrix} x_s - x_u & \dot{x}_s & x_u - x_r & \dot{x}_u \end{bmatrix}^{\mathrm{T}}, \tag{8}$$

$$\omega = \dot{x}_r, \tag{9}$$

$$u = u_z \tag{10}$$

The performance output is defined by the vertical acceleration $\ddot{x}_s$, by which the ride comfort performance is evaluated, that is

$$z_1 = \ddot{x}_s \tag{11}$$

The performance requirements of (4)–(6) do not need to be minimized and should be designed as hard constraints. Thus, the constrained output of the active suspension system consists of the normalized suspension stroke, the road-holding, and the actuator saturation constraints, that is

$$z_2 = \begin{bmatrix} \frac{x_s - x_u}{S_{\max}} & \frac{k_u(x_u - x_r)}{(m_s + m_u)g} & \frac{u_z}{u_{z\max}} \end{bmatrix}^{\mathrm{T}} \tag{12}$$

Since the state variables of the active suspension system cannot be fully measured in practice, the suspension stroke and the sprung mass velocity are taken as the feedback quantities. The suspension stroke can be directly measured by displacement sensors, and the sprung mass velocity can be obtained by the body acceleration sensors (Du and Zhang, 2008). Then the measurement output is

$$y = [x_s - x_u \quad \dot{x}_s]^{\mathrm{T}} \tag{13}$$

The matrices in active suspension system (7) are

$$A = \begin{bmatrix} 0 & 1 & 0 & -1 \\ -\frac{k_s}{m_s} & -\frac{c_s}{m_s} & 0 & \frac{c_s}{m_s} \\ 0 & 0 & 0 & 1 \\ \frac{k_s}{m_u} & \frac{c_s}{m_u} & -\frac{k_u}{m_u} & -\frac{c_s}{m_u} \end{bmatrix},$$

$$B_1 = \begin{bmatrix} 0 & 0 & -1 & 0 \end{bmatrix}^{\mathrm{T}},$$

$$B_2 = \begin{bmatrix} 0 & \frac{1}{m_s} & 0 & -\frac{1}{m_u} \end{bmatrix}^{\mathrm{T}},$$

$$C_1 = \begin{bmatrix} -\frac{k_s}{m_s} & -\frac{c_s}{m_s} & 0 & \frac{c_s}{m_s} \end{bmatrix},$$

$$C_2 = \begin{bmatrix} \frac{1}{S_{\max}} & 0 & 0 & 0 \\ 0 & 0 & \frac{k_u}{(m_s + m_u)g} & 0 \\ 0 & 0 & 0 & 0 \end{bmatrix},$$

$$C_3 = \begin{bmatrix} 1 & 0 & 0 & 0 \\ 0 & 1 & 0 & 0 \end{bmatrix},$$

$$D_{11} = 0, \quad D_{12} = \frac{1}{m_s},$$

$$D_{21} = \begin{bmatrix} 0 & 0 & 0 \end{bmatrix}^{\mathrm{T}}, \quad D_{22} = \begin{bmatrix} 0 & 0 & \frac{1}{u_{z\max}} \end{bmatrix}^{\mathrm{T}},$$

where $D_{21} = \mathbf{0}$ is supposed, that is, the disturbance input does not directly affect the constrained output of the system.

The active suspension control can be described as a multi-objective control problem with time-domain hard constraints. And the control objectives include improving ride comfort, that is, minimizing the response from the road disturbance to the vertical acceleration of the vehicle body. Meanwhile, the time-domain hard constraints should be satisfied.

3. H_∞/GH_2 static output feedback control

In this section, H_∞ norm and GH_2 norm are introduced to describe the performance output and the constrained output, respectively. And the H_∞/GH_2 static output feedback controller is designed.

3.1. H_∞ norm and GH_2 norm

Suppose the static output feedback control is

$$u(t) = Fy(t) \tag{14}$$

where $F \in \mathbb{R}^{n_u \times n_y}$ is the matrix to be determined. Substitute $u(t) = Fy(t)$ into (7), then the closed-loop system is obtained, that is

$$\begin{cases} \dot{x}(t) = A_{cl}x(t) + B_{cl}\omega(t), \\ z_1(t) = C_{1,cl}x(t) + D_{1,cl}\omega(t), \\ z_2(t) = C_{2,cl}x(t) + D_{2,cl}\omega(t), \end{cases} \tag{15}$$

where

$$A_{cl} = A + B_2FC_3,$$

$$C_{1,cl} = C_1 + D_{12}FC_3,$$

$$C_{2,cl} = C_2 + D_{22}FC_3,$$

$$B_{cl} = B_1,$$

$$D_{1,cl} = D_{11},$$

$$D_{2,cl} = D_{21}$$

Define the H_∞ norm of system (15) from disturbance input ω to performance output z_1 as

$$\|T_{\omega z_1}\|_\infty := \sup_{\omega(t)\in L_2} \frac{\|z_1(t)\|_2}{\|\omega(t)\|_2} \tag{16}$$

where $\omega(t) \in L_2$ indicates that the disturbance input is an energy-bounded signal, that is

$$\|\omega(t)\|_2 := \sqrt{\int_0^\infty \|\omega(t)\|^2 dt} < \infty \tag{17}$$

The H_∞ norm is the peak value of the maximum singular value of the system frequency response. When the input energy is bounded, the H_∞ norm describes the ratio of the system output signal energy to the input signal energy. The smaller the H_∞ norm is, the less the disturbance input of the system influences the performance output.

Lemma 1. (Boyd et al., 1994; Schereret and Weiland, 2011) For system (15), given a real number $\gamma > 0$, then the following conditions are equivalent

1. The system is asymptotically stable and $\|T_{\omega z_1}\|_\infty < \gamma$;
2. There exists a matrix $P_1 = P_1^T > 0$ such that

$$\begin{bmatrix} A_{cl}^T P_1 + P_1 A_{cl} & \# & \# \\ B_{cl}^T P_1 & -I & \# \\ C_{1,cl} & D_{1,cl} & -\gamma^2 I \end{bmatrix} < 0 \tag{18}$$

Assuming that $x(0) = \mathbf{0}$, the GH_2 norm of the system from the disturbance input ω to the output z_2 is

$$\|T_{\omega z_2}\|_g := \sup_{\omega(t)\in L_2} \frac{\|z_2(t)\|_\infty}{\|\omega(t)\|_2} \tag{19}$$

When ω is a unit energy signal, the GH_2 norm represents the peak of the constrained output in the time domain.

Lemma 2. (Boyd et al., 1994; Schereret and Weiland, 2011) Suppose that $D_{21} = \mathbf{0}$ and $x(0) = \mathbf{0}$, for system (15), the following conditions are equivalent

1. The system is asymptotically stable and $\|T_{\omega z_2}\|_g < 1$;
2. There exists a matrix $P_2 = P_2^T > 0$ such that

$$\begin{bmatrix} A_{cl}^T P_2 + P_2 A_{cl} & \# \\ B_{cl}^T P_2 & -I \end{bmatrix} < 0 \tag{20a}$$

$$\begin{bmatrix} P_2 & \# \\ C_{2,cl} & I \end{bmatrix} > 0 \tag{20b}$$

3.2. Static output feedback controller design

H_∞/GH_2 static output feedback controller is to design the static output feedback gain F such that

1. The closed-loop system (15) is internally stable;
2. When the disturbance input is an energy-bounded signal, the H_∞ norm $\|T_{\omega z_1}\|_\infty$ from the disturbance input $\omega(t)$ to the performance output $z_1(t)$ is minimum and the GH_2 norm from $\omega(t)$ to the constrained output $z_2(t)$ satisfies $\|T_{\omega z_2}\|_g < 1$.

In order to transform the control problem into a convex optimization problem that can be solved by LMIs, the following lemma is first introduced.

Lemma 3. Given a positive definite symmetric matrix $S \in \mathbb{R}^{n\times n}$ and a full row rank matrix $N \in \mathbb{R}^{m\times n}$ with $m \le n$, the matrix NSN^T is invertible.

Proof. Let the vector be $X \in \mathbb{R}^m$ such that $NSN^T X = \mathbf{0}$, then $X^T NSN^T X = 0$, that is, $(N^T X)^T S (N^T X) = 0$. Furthermore, $N^T X = \mathbf{0}$ since S is a positive definite symmetric matrix. Multiplying N left on both sides of the equation, $NN^T X = \mathbf{0}$ is obtained. As NN^T is invertible, then $X = \mathbf{0}$. In summary, $NSN^T X = \mathbf{0}$ has only zero solutions, that is, NSN^T is invertible.

The theorem for solving the H_∞/GH_2 static output feedback gain F is given below.

Theorem 1. Suppose there exist matrix $U \in \mathbb{R}^{n_u \times n_y}$, positive definite symmetries matrix $Q \in \mathbb{R}^{n_x \times n_x}$, and the scalar $\gamma > 0$ such that the following LMIs optimization problem

$$\underset{\gamma, Q, U}{\text{minimize}} \quad \gamma^2, \tag{21a}$$

subject to

$$\begin{bmatrix} AQ + QA^T + B_2UC_3 + (B_2UC_3)^T & \# & \# \\ B_1^T & -I & \# \\ C_1Q + D_{12}UC_3 & D_{11} & -\gamma^2 I \end{bmatrix} < 0, \tag{21b}$$

$$\begin{bmatrix} Q & \# \\ C_2Q + D_{22}UC_3 & I \end{bmatrix} > 0 \tag{21c}$$

has the optimal solution (γ^*, Q^*, U^*), $F^* = U^*(V^*)^{-1}$, and $V^* = (C_3Q^*C_3^T)(C_3C_3^T)^{-1}$, the closed-loop system (15) with the static output feedback control $u = F^* y$ satisfies

1. Internal stability;
2. The H_∞ performance from the road disturbance $\omega(t)$ to the performance output $z_1(t)$ is less than γ^*, and the GH_2 norm from $\omega(t)$ to the output $z_2(t)$ is less than 1.

Proof. According to Lemma 1 and Lemma 2, in a multi-objective control framework, the conditions that A_{cl} is internally stable, $\|T_{\omega z_1}\|_\infty < \gamma$ and $\|T_{\omega z_2}\|_g < 1$ can be deduced to there exist matrices $P_1 = P_1^T > 0$ and $P_2 = P_2^T > 0$ such that

$$\begin{bmatrix} A_{cl}^{\mathrm{T}} P_1 + P_1 A_{cl} & \# & \# \\ B_{cl}^{\mathrm{T}} P_1 & -I & \# \\ C_{1,cl} & D_{1,cl} & -\gamma^2 I \end{bmatrix} < 0 \tag{22a}$$

$$\begin{bmatrix} A_{cl}^{\mathrm{T}} P_2 + P_2 A_{cl} & \# \\ B_{cl}^{\mathrm{T}} P_2 & -I \end{bmatrix} < 0 \tag{22b}$$

$$\begin{bmatrix} P_2 & \# \\ C_{2,cl} & I \end{bmatrix} > 0 \tag{22c}$$

Let the matrix $P_1 = P_2 = P$, then substitute A_{cl}, B_{cl}, $C_{1,cl}$, $C_{2,cl}$, $D_{1,cl}$, and P into the matrix inequalities (22a) and (22c), there are

$$\begin{bmatrix} (A + B_2 F C_3)^{\mathrm{T}} P + P(A + B_2 F C_3) & \# & \# \\ B_1^{\mathrm{T}} P & -I & \# \\ C_1 + D_{12} F C_3 & D_{11} & -\gamma^2 I \end{bmatrix} < 0, \tag{23a}$$

$$\begin{bmatrix} P & \# \\ C_2 + D_{22} F C_3 & I \end{bmatrix} > 0 \tag{23b}$$

Note that the linear matrix inequality (22b) is intrinsic to (22a).

Let $Q = P^{-1}$, multiply inequality (23a) left and right by diag $\{Q, I, I\}$, and multiply inequality (23b) left and right by diag $\{Q, I\}$, respectively, to obtain

$$\begin{bmatrix} AQ + QA^{\mathrm{T}} + B_2 F C_3 Q + (B_2 F C_3 Q)^T & \# & \# \\ B_1^{\mathrm{T}} & -I & \# \\ C_1 Q + D_{12} F C_3 Q & D_{11} & -\gamma^2 I \end{bmatrix} < 0, \tag{24a}$$

$$\begin{bmatrix} Q & \# \\ C_2 Q + D_{22} F C_3 Q & I \end{bmatrix} > 0 \tag{24b}$$

Denote $V = (C_3 Q C_3^{\mathrm{T}})(C_3 C_3^{\mathrm{T}})^{-1}$, that is, $V C_3 C_3^{\mathrm{T}} = C_3 Q C_3^{\mathrm{T}}$, or $(V C_3 - C_3 Q) C_3^{\mathrm{T}} = 0$, where $C_3^{\mathrm{T}} \in \mathbb{R}^{n_x \times n_y}$ and $(V C_3 - C_3 Q) \in \mathbb{R}^{n_y \times n_x}$. Since $C_3 \in \mathbb{R}^{n_y \times n_x}$ and $n_y \le n_x$, the maximum value of rank$(V C_3 - C_3 Q)$ is n_y. Because $(V C_3 - C_3 Q)X = 0$ has n_y non-zero solutions, there is $V C_3 = C_3 Q$. According to Lemma 3, $C_3 Q C_3^{\mathrm{T}}$ is invertible, so is V invertible.

Taking $V C_3 = C_3 Q$ and $F = U V^{-1}$ into matrix inequalities (24a) and (24b), the linear matrix inequalities (21b) and (21c) can be obtained. Suppose the optimization problem (21) is solved with an optimal solution (γ^*, Q^*, U^*), then the conclusions (1)–(2) are satisfied in the closed-loop system (15).

Remark. For the external disturbance not exceeding unit energy, that is, $\|\omega(t)\|_2 \le 1$, the hard constraints are satisfied when condition (2) above is satisfied.

4. Simulation and HiL experiments

This section presents comparative experiments of active suspension between the proposed approach and the existing approaches, such as H_∞ state feedback control (Du and Zhang, 2007) and GAs active suspension which utilizes LMIs and GAs (Du and Zhang, 2008). Both simulation and HiL experiments are conducted on active and passive suspensions under different road disturbances and vehicle speeds, illustrating the superiority of the proposed H_∞/GH_2 static output feedback control to achieve better ride comfort with less feedback quantities and without need for a searching algorithm. The parameters are shown in Table 1 (Gordon et al., 1991).

4.1. Road disturbance

The deterministic road is represented by an isolated bump in an otherwise smooth road surface, that is, (Chen and Guo, 2005; Chen et al., 2007)

$$x_r(t) = \begin{cases} \dfrac{A_m}{2}\left(1 - \cos\dfrac{2\pi v}{L} t\right), & 0 \le t \le \dfrac{L}{v}, \\ 0, & t > \dfrac{L}{v}, \end{cases} \tag{25}$$

where v and t are the vehicle velocity and time, respectively, the height and length of the bump are A_m and L, respectively.

The random process with power spectral density (PSD) of Du et al. (2020) is taken for the random road (ISO 8608, 1995)

$$G_{xr}(n) = G_{xr}(n_0)\left(\frac{n}{n_0}\right)^{-\omega_0} \tag{26}$$

where $G_{xr}(n)$ is PSD with the spatial frequency n and $G_{xr}(n_0)$ is the spectral density with the reference spatial frequency $n_0 = 0.1\ \mathrm{m}^{-1}$. The variable ω_0 is frequency index which stands for the frequency structure of PSD. In this paper, the frequency index is chosen as $\omega_0 = 2$, and the ground velocity can be generated by a white-noise signal

$$\dot{x}_r(t) = -2\pi n_1 v x_r(t) + 2\pi n_0 \sqrt{G_{xr}(n_0) v}\,\omega(t) \tag{27}$$

where $n_1 = 0.01$, and $\omega(t)$ is a Gaussian white-noise with a zero mean value and an intensity of 1. According to the grade of road roughness, the geometric mean values of

Table 1. Parameters of suspension and road.

Parameters	Symbol	Simulation	HiL	Unit
Sprung mass	m_s	320	2.45	kg
Unsprung mass	m_u	40	1	kg
Tire stiffness	k_u	200,000	2500	N/m
Spring stiffness	k_s	18,000	900	N/m
Damping coefficient	c_s	1000	7.5	N · s/m
Maximum active force	$u_{z\ max}$	1000	25	N
Maximum suspension stroke	S_{max}	0.08	0.03	m
Bump height	A_m	0.1	5	m
Bump length	L	0.032	1	m

$G_{xr}(n_0)$ for commonly used B class and C class road are 64×10^{-6} and 256×10^{-6}, respectively.

4.2. Simulation results

By solving the convex optimization problem (21), the results of proposed H_∞/GH_2 static output feedback controller gains F^* and H_∞ performance γ^* are obtained as

$$F^* = [-18944 \quad -4535], \quad \gamma^* = 0.7152 \tag{28}$$

For comparison, a H_∞ state feedback control is designed to minimize conflicting performance requirements in a single objective function (Du and Zhang, 2007). Suppose that the system state variables are measurable in simulation, the controlled output $z_z(t)$ is composed of $\ddot{x}_s$, $x_s - x_u$, $x_u - x_r$ and u_z. The control system is

$$\begin{cases} \dot{x}(t) = Ax(t) + B_1\omega(t) + B_2u(t), \\ z_z(t) = C_{z1}x(t) + D_{z1}\omega(t) + D_{z2}u(t), \\ y_z(t) = C_{z2}x(t), \end{cases} \tag{29}$$

where $x(t)$, $\omega(t)$, A, B_1, and B_2 are defined as system (7), $u(t)$ is the control input, $y_z(t)$ is the measured output, with

$$C_{z1} = \begin{bmatrix} -\frac{k_s}{m_s} & -\frac{c_s}{m_s} & 0 & \frac{c_s}{m_s} \\ \kappa_1 & 0 & 0 & 0 \\ 0 & 0 & \kappa_2 & 0 \\ 0 & 0 & 0 & 0 \end{bmatrix}, \quad C_{z2} = I_{4\times4}$$

$$D_{z1} = \begin{bmatrix} 0 \\ 0 \\ 0 \\ 0 \end{bmatrix}, \quad D_{z2} = \begin{bmatrix} \frac{1}{m_s} \\ 0 \\ 0 \\ \kappa_3 \end{bmatrix},$$

where $\kappa_1 = 5/S_{\max}$, $\kappa_2 = k_u/((m_s + m_u)g)$, and $\kappa_3 = 8/u_{\max}$ are weightings for the performance of suspension stroke, road-holding, and actuator saturation, respectively. The design of H_∞ state feedback control is to find a state feedback control $u_k(t) = K_z x(t)$ such that the system is asymptotically stable and the H_∞ norm of system (29) from disturbance input ω to controlled output z_z is minimized.

The simulations are performed with both isolated bump excitation and random road disturbance input. Due to the page limit, partial results are presented in Figures 2 and 3, where the solid red lines indicate the response curves of the active suspension with proposed H_∞/GH_2 static output feedback controller (named as H_∞/GH_2 active suspension), the dotted green lines and dashed dot blue lines indicate H_∞ state feedback control (named as H_∞ active suspension) and GAs active suspension, respectively, the dashed black lines represent the response curves of passive suspension, and the dotted black lines indicate the maximum and minimum values of suspension stroke and active force.

The simulation results of isolated bump excitation with v = 50 km/h are shown in Figure 2, the sampling time is 0.02 s. As shown in Figure 2(a), the amplitude of $\ddot{x}_s$ for the H_∞/GH_2 active suspension is the smallest among suspensions, and the convergence time is shorter than that of the passive suspension, indicating that the proposed controller is effective in improving ride comfort. Moreover, Figure 2(b) shows that the passive suspension stroke exceed S_{max}, which implies mechanical damage in the actual system. Compared with the H_∞ state feedback control which requires the system state to be fully measurable and the active suspension controller which uses the searching algorithm such as GAs, the proposed H_∞/GH_2 active suspension can perform superior ride comfort.

The simulation results on B class random roads with v = 100 km/h are presented in Figure 3, all the active suspensions are optimized to minimize $\ddot{x}_s$ while satisfying time-domain hard constraints compared to the passive suspension.

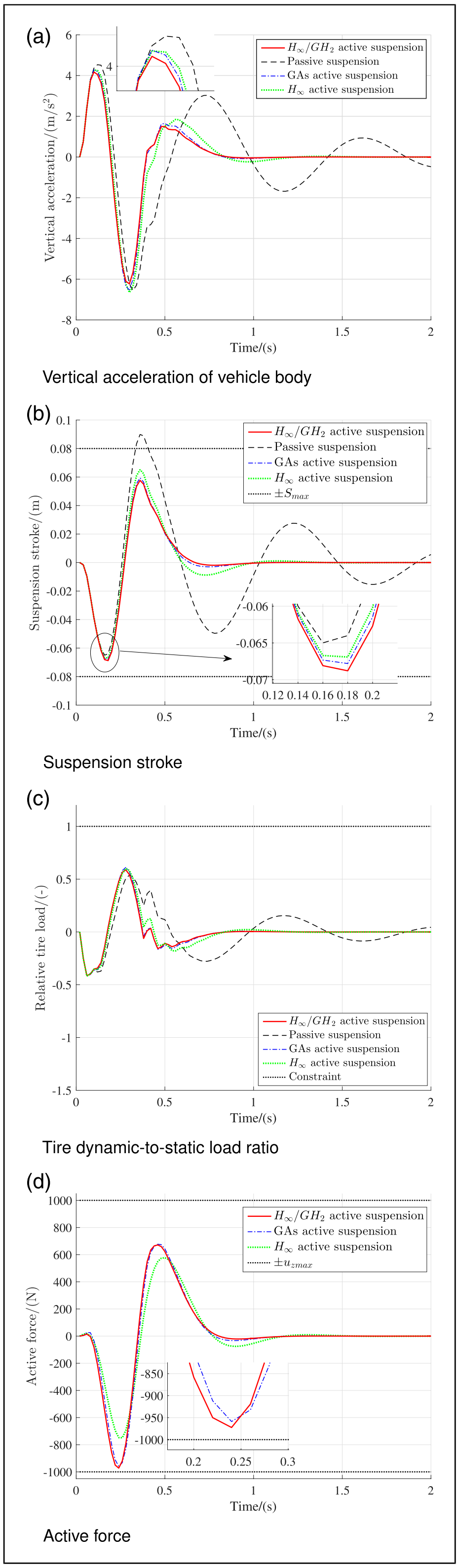

Figure 2. Suspension response on bump road (v = 50 km/h).

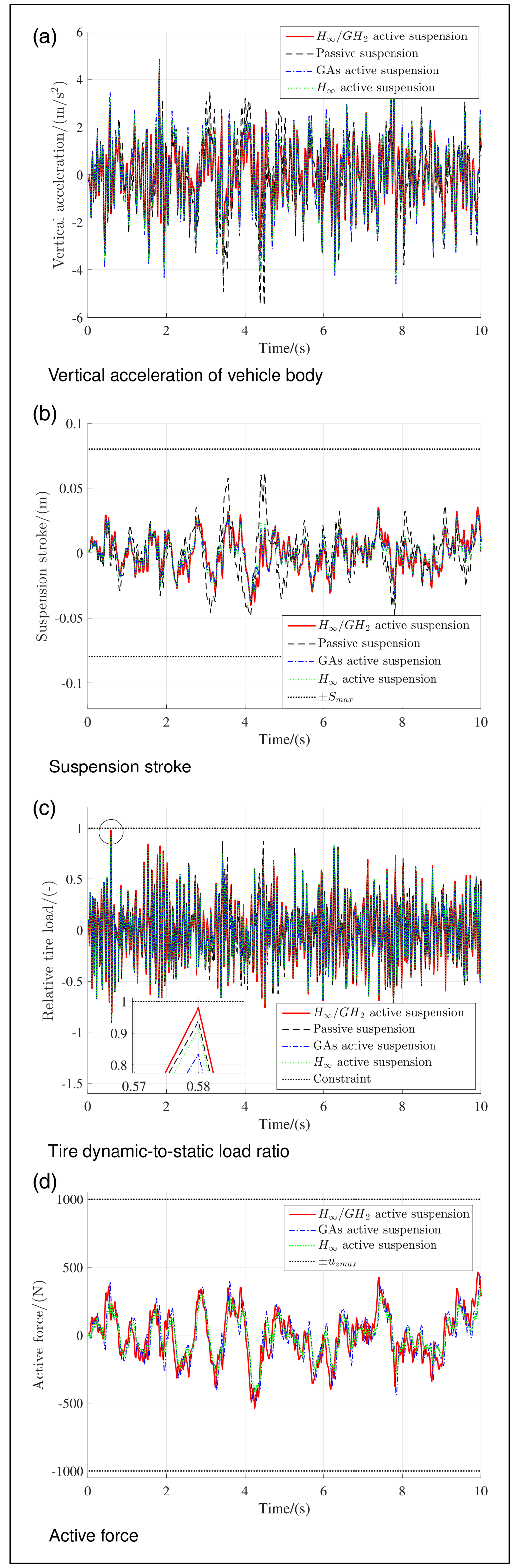

Figure 3. Suspension response on B class road (v = 100 km/h).

Table 2. RMS values of vehicle body vertical acceleration (m/s^2) in simulation.

Suspension	Bump 50(km/h)	Bump 30(km/h)	B class 100(km/h)	C class 45(km/h)
H_∞/GH_2	1.6806	1.3132	1.3361	1.1184
H_∞	1.8278	1.5560	1.4716	1.2409
GAs	1.7610	1.5594	1.5530	1.2960
Passive	2.2517	2.5147	1.6398	1.3785

Table 3. Reduction of RMS values by H_∞/GH_2 active suspension in simulation.

Suspension	Bump 50(km/h)	Bump 30(km/h)	B class 100(km/h)	C class 45(km/h)
H_∞	8.1%	15.6%	9.2%	9.9%
GAs	4.6%	15.8%	14.0%	13.7%
Passive	25.4%	47.8%	18.5%	18.9%

To quantitatively evaluate the effectiveness of the proposed approach in improving ride comfort, RMS values of $\ddot{x}_s$ are shown in Table 2, and the percentages of RMS values reduced by H_∞/GH_2 control compared to other control methods are shown in Table 3. In addition, to evaluate the amplitude of $\ddot{x}_s$ on bump roads, peak-to-peak (P2P) values are calculated and shown in Table 4.

As can be seen in Tables 2–4, the proposed H_∞/GH_2 active suspension exhibits the most optimal ride comfort performance. Compared to H_∞ state feedback control, H_∞/GH_2 static output feedback control is able to reduce RMS values by at least 8.1% and satisfy all time-domain hard constraints. This is because the H_∞ state feedback control optimizes conflicting performance requirements in a single objective function, making the control problem conservative to a certain extent.

4.3. HiL experiments

In this subsection, comparative HiL experiments are conducted to further demonstrate the practical effectiveness of the proposed approach.

HiL experiments are conducted based on the active suspension test platform developed by Quanser® company in Canada (Apkarian and Abdossalami, 2013), as shown in Figure 4.

The test platform mainly includes the active suspension system, displacement and acceleration sensors, a power amplifier, a data acquisition (DAQ) device, and a computer.

Table 4. P2P values of vehicle body vertical acceleration (m/s^2) on bump roads.

Suspension	v = 50(km/h)	v = 30(km/h)
H_∞/GH_2	10.40	5.00
H_∞	10.92	7.05
GAs	10.81	7.18
Passive	11.09	10.18

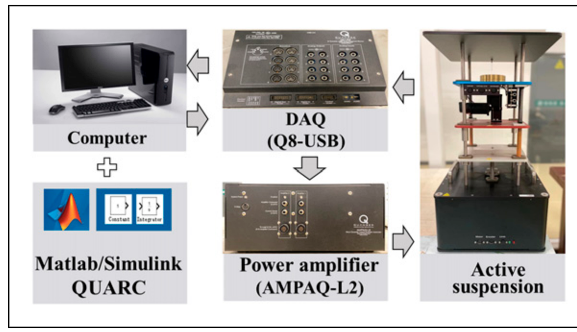

Figure 4. The active suspension test platform.

The output signals suspension stroke and sprung mass velocity are obtained by a US Digital S1 single-ended optical shaft encoder and a dual-axis ADXL210 E accelerometer, respectively, with the sampling frequency 50 Hz. And the active force is generated by a high quality DC motor. The computer conducts controller design and data processing through Matlab/Simulink and the software QUARC®. The control signals are sent to the active suspension system through the DAQ device and the power amplifier, while the feedback signals are received to complete the closed-loop control.

The controller gains and H_∞ performance are

$$F^* = [-561.59 \quad -53.03], \quad \gamma^* = 10.07 \tag{30}$$

Due to the page limit, partial results with isolated bump road and random roads are presented in Figures 5 and 6, the legends are consistent with that in Figure 2.

The simulation results of bump road with $v = 11$ km/h are shown in Figure 5. As shown in Figure 5(a), the vertical acceleration amplitude and the convergence time of the proposed H_∞/GH_2 active suspension are smallest among three suspensions. Moreover, the dynamic-to-static load ratio of passive suspension exceeds the constraint (c.f. Figure 5(c)). On the contrary, the H_∞/GH_2 active suspension satisfies all time-domain constraints (c.f. Figures 5(b)–(d)).

Additionally, HiL experiments with B class and C class roads are conducted with v = 120 km/h and v = 90 km/h,

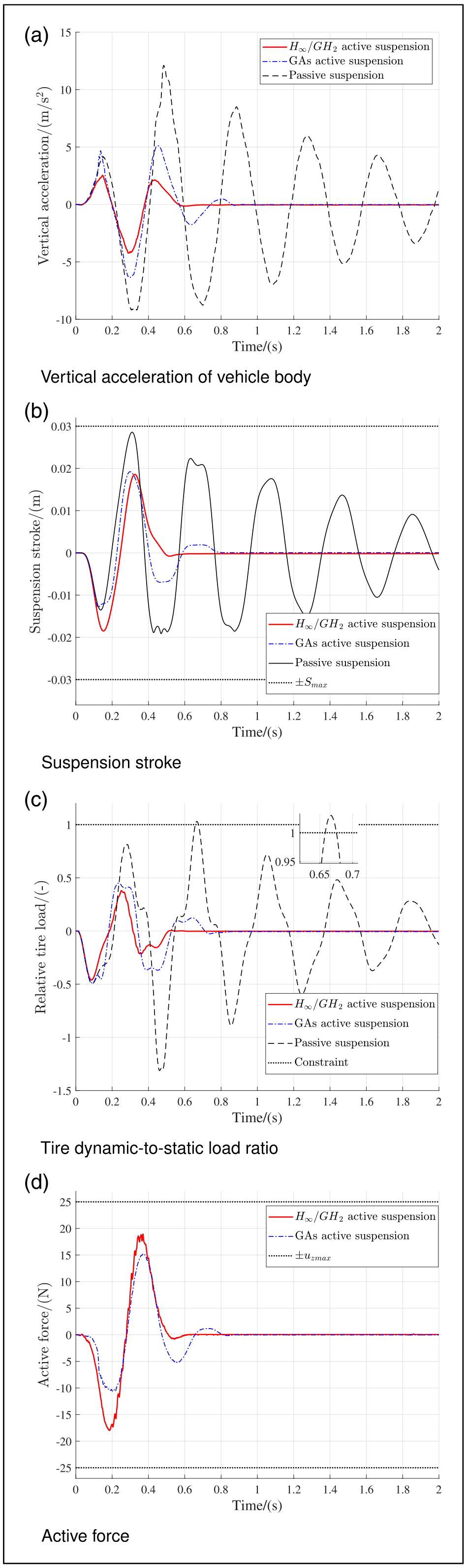

Figure 5. Suspension response on bump road (v = 11 km/h).

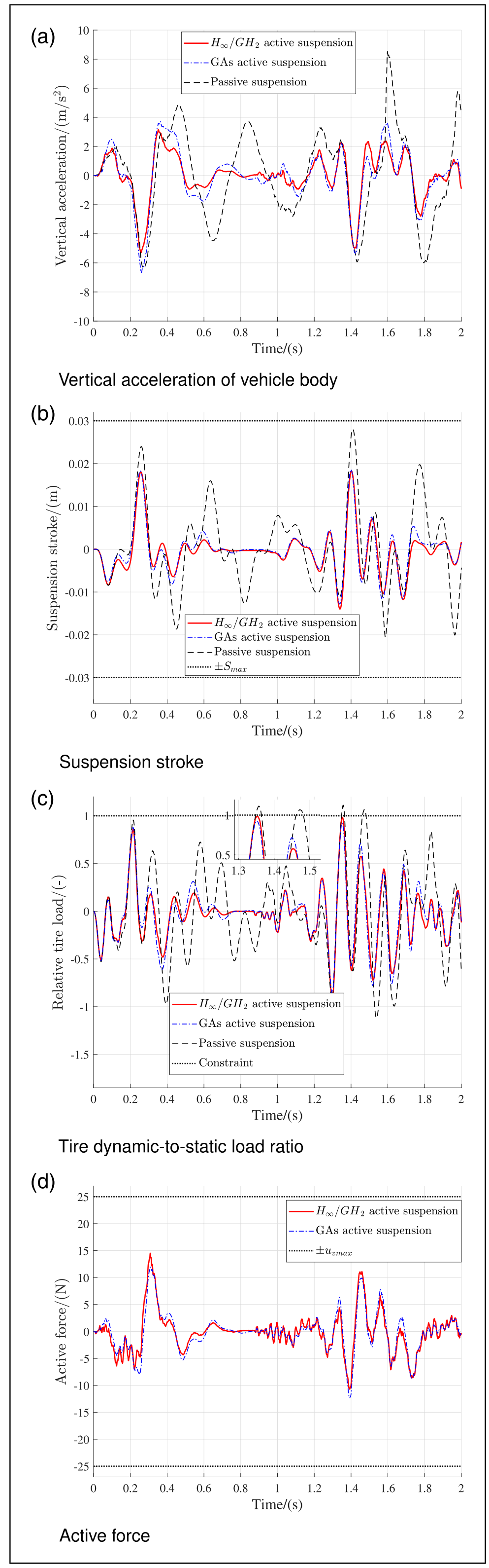

Figure 6. Suspension response on C class road (v = 90 km/h).

Table 5. RMS values of vehicle body vertical acceleration (m/s^2) in HiL experiments.

Suspension	Bump 10(km/h)	Bump 11(km/h)	B class 120(km/h)	C class 90(km/h)
H_∞/GH_2	1.2618	1.5413	0.9912	1.5205
GAs	1.6831	1.7949	1.0961	1.8937
Passive	4.3020	5.8353	2.0772	3.0078

Table 6. Reduction of RMS values by H_∞/GH_2 active suspension in HiL experiments.

Suspension	Bump 10(km/h)	Bump 11(km/h)	B class 120(km/h)	C class 90(km/h)
GAs	25.0%	14.1%	9.6%	19.7%
Passive	70.7%	73.6%	52.3%	49.5%

Table 7. P2P values of vehicle body vertical acceleration (m/s^2) on bump roads.

Suspension	v = 10(km/h)	v = 11(km/h)
H_∞/GH_2	5.68	6.77
GAs	11.82	11.47
Passive	16.65	21.24

Table 8. Controller gains and H_∞ performance of GAs active suspension in HiL experiments.

Road	Speed(km/h)	F	γ
Bump	10	[−762.6 −68.8]	3.2671
Bump	11	[−261.4 −47.5]	3.2747
B class	120	[−543.8 −43.5]	3.4233
C class	90	[−649.2 −32.9]	3.4530

respectively. The results of the C class road are presented in Figure 6, where the tire dynamic-to-static load ratio of passive suspension (dotted black lines) exceeds the constraint, while the H_∞/GH_2 active suspension (solid red lines) can reduce the vertical acceleration of the vehicle body and meet the constraints.

Remark. The control gains of GAs active suspension are largely influenced by the search space and iteration numbers of search algorithm GAs. Since the suspension parameters are different in simulation and HiL experiments, the search space and the solutions are different. Thus the deviations between the active forces in Figure 2(d) and Figure 5(d) are different.

The RMS values of $\ddot{x}_s$ are shown in Table 5, and the RMS values reduction percentage of H_∞/GH_2 active suspension compared to those of GAs active suspension and passive suspension are shown in Table 6. Moreover, P2P values of bump roads are shown in Table 7. As shown in tables, the proposed approach can greatly reduce RMS and P2P values of $\ddot{x}_s$ and improve ride comfort.

The controller gains and H_∞ performance of GAs active suspension are presented in Table 8. Note that the controller gains are obtained within the search space of [−1000, −200] and [−70, −30], which are set based on the existing optimal solution in (30). Careful selection of the search space is a necessary factor to obtain the suboptimal solution. However, the proposed approach does not require extensive searching while ensuring system performance.

To further illustrate the impact of different search spaces and randomness of GAs, repeated experiments are conducted on a C class road surface with v = 90 km/h. The results are listed in Table 9, the search space of the first four experiments contains the optimal feedback control gain F^*. As can be seen in Table 9, all the RMS values are larger than that obtained by the proposed approach. Moreover, the search space of the last two experiments does not contain F^*, resulting in the controller gain is far from the optimal

Table 9. Results of repeated HiL experiments on C class road surface with v = 90 km/h.

Number	Search space of F_1 and F_2	F_1, F_2	γ	RMS (m/s^2)
1	[−1000, −200], [−70, −30]	−976.2, −37.3	3.2839	1.9101
3	[−1000, −200], [−70, −30]	−438.2, −44.3	3.6729	1.6433
4	[−1000, −200], [−120, −20]	−995.5, −52.2	2.7537	1.8818
5	[−800, −200], [−40, −10]	−342.9, −31.2	6.6355	1.6741
6	[−1000, −600], [−40, −10]	−883.4, −29.2	10.8530	2.1626

value, and RMS values are large. The average RMS value of the six experiments is 1.8390, which is larger than the RMS value of 1.5205 obtained by the proposed approach.

5. Conclusion

In this paper, the multi-objective control problem with time-domain hard constraints for active suspension was transformed into a convex optimization problem that can be solved using LMIs. The H_∞ norm and the GH_2 norm were used to describe the optimization index and the hard constraints of the active suspension system, respectively. A static output feedback control was designed using measurable suspension stroke and sprung mass velocity as the feedback quantities. Comparative experiments were conducted with both determined and random road disturbances by simulation and HiL experiments. The experiment results showed the superiority of the proposed approach over the H_∞ state feedback control approach and the approach that relies on LMIs and searching algorithm in terms of enhancing ride comfort. Furthermore, the proposed approach can effectively meet all time-domain hard constraints.

Declaration of conflicting interests

The author(s) declared no potential conflicts of interest with respect to the research, authorship, and/or publication of this article.

Funding

The author(s) disclosed receipt of the following financial support for the research, authorship, and/or publication of this article: This work was supported by the National Natural Science Foundation (NNSF) of China under Grant (No. U1964202), the Natural Science Foundation of Jilin Province (No. YDZJ202101-ZYTS169), and the Foundation of Key Laboratory of Industrial Internet of Things and Networked Control (No. 2019FF01).

ORCID iDs

Zhuqing Shi https://orcid.org/0000-0002-5110-2782
Shishuo Zhang https://orcid.org/0009-0002-2133-6630

References

Akbari A, Geravand M and Lohmann B (2010) Output feedback constrained H_∞ control of active vehicle suspensions. In: 2010 2nd International Conference on Advanced Computer Control, 27–29 March 2010, Shenyang, China, Vol. 3, pp. 399–404. IEEE.

Apkarian J and Abdossalami A (2013) *Active Suspension Experiment for MATLAB/Simulink Users-Laboratory Guide*. Markham, Ontario, Canada: Quanser Inc.

Boyd S, El Ghaoui L, Feron E, et al. (1994) *Linear Matrix Inequalities in System and Control Theory*. Philadelphia, PA: Society for industrial and applied mathematics.

Camino JF, Zampieri DE and Peres PL (1999) Design of a vehicular suspension controller by static output feedback. In: Proceedings of the 1999 American Control Conference (Cat. No. 99CH36251), 02–04 June 1999, San Diego, CA, USA, Vol. 5, pp. 3168–3172. IEEE.

Chen H and Guo KH (2005) Constrained H_∞ control of active suspensions: an LMI approach. *IEEE Transactions on Control Systems Technology* 13(3): 412–421.

Chen H, Sun PY and Guo K-H (2003) A multi-objective control design for active suspensions with hard constraints. In: Proceedings of the 2003 American Control Conference, 4–6 June 2003, Dever, Colorado, Vol. 5, pp. 4371–4376. IEEE.

Chen H, Ma MM and Sun PY (2007) H_2/generalized H_2 output feedback control for active suspension. *Control Theory & Applications* 24(5): 790–794.

Deshpande VS, Shendge PD and Phadke SB (2017) Nonlinear control for dual objective active suspension systems. *IEEE Transactions on Intelligent Transportation Systems* 18(3): 656–665.

Du H and Zhang N (2007) H_∞ control of active vehicle suspensions with actuator time delay. *Journal of Sound and Vibration* 301: 236–252.

Du H and Zhang N (2008) Designing H_∞/GH_2 static-output feedback controller for vehicle suspensions using linear matrix inequalities and genetic algorithms. *Vehicle System Dynamics* 46(5): 385–412.

Du M, Zhao D, Yang M, et al. (2020) Nonlinear extended state observer-based output feedback stabilization control for uncertain nonlinear half-car active suspension systems. *Nonlinear Dynamics* 100(1): 2483–2503.

Gordon TJ, Marsh C and Milsted MG (1991) A comparison of adaptive LQG and nonlinear controllers for vehicle suspension systems. *Vehicle System Dynamics* 20(6): 321–340.

Goyal JK, Aggarwal S, Sachan A, et al. (2023) An improved output feedback controller design for linear discrete-time systems using a matrix decomposition method. *Asian Journal of Control* 25(2): 769–782.

ISO 8608 (1995) Mechanical vibration-road surface profiles-reporting of measured data, 1995.

Kim Y, Kwak T, Kanno M, et al. (2023) Multi-objective finite-frequency H_∞/GH_2 static output-feedback control synthesis for full-vehicle active suspension systems: a metaheuristic optimization approach. *IEEE Access* 11: 36309–36330.

Li WF, Xie ZC, Wong PK, et al. (2019) Robust nonfragile H_∞ optimum control for active suspension systems with time-varying actuator delay. *Journal of Vibration and Control* 25(18): 2435–2452.

Liu S-B and Zhao D-X (2009) H_∞/Generalized H_2 static output feedback control method for active suspension. *China Journal of Highway and Transport* 22(4): 122.

Park M and Yim S (2021) Design of static output feedback and structured controllers for active suspension with quarter-car model. *Energies* 14(24): 8231.

Scherer C and Weiland S (2011) Linear matrix inequalities in control. In: Levine WS (ed). *The Control Systems Handbook*. 2nd edition. Boca Raton, FL: CRC Press, 24.1–24.30.

Song S and Wang J (2020) Incremental model predictive control of active suspensions with estimated road preview information from a lead vehicle. *Journal of Dynamic Systems, Measurement, and Control* 142(12).

Taghirad HD and Esmailzadeh E (1998) Automobile passenger comfort assured through LQG/LQR active suspension. *Journal of Vibration and Control* 4(5): 603–618.

Theunissen J, Sorniotti A, Gruber P, et al. (2020) Regionless explicit model predictive control of active suspension systems with preview. *IEEE Transactions on Industrial Electronics* 67(6): 4877–4888.

Tseng HE and Hrovat D (2015) State of the art survey: active and semi-active suspension control. *Vehicle System Dynamics* 53(7): 1034–1062.

Wang J, Jin F, Zhou L, et al. (2019) Implementation of model-free motion control for active suspension systems. *Mechanical Systems and Signal Processing* 119: 589–602.

Wei C, Zhang K, Cai Y, et al. (2018) A new method of static output-feedback H_∞ controller design for 5 DOF vehicle active suspension system. *Journal of the Brazilian Society of Mechanical Sciences and Engineering* 40: 1–12.

Wei C, Cai Y, Zhang K, et al. (2020) Novel optimal design approach for output-feedback H_∞ control of vehicle active seat-suspension system. *Asian Journal of Control* 22(1): 411–422.

Zhang H, Zhang Y, Yu X, et al. (2022) Improved LQG vibration control for multiple inputs of electric vehicle. *Advances in Mechanical Engineering* 14(1): 166–179. doi: 10.1177/16878140211072942